

# Heavy flavor jet production and substructure in electron-nucleus collisions

Hai Tao Li<sup>a,b,c</sup>, Ze Long Liu<sup>c</sup>, Ivan Vitev<sup>c</sup>

<sup>a</sup>*School of Physics, Shandong University, Jinan, Shandong 250100, China*

<sup>b</sup>*HEP Division, Argonne National Laboratory, Argonne, Illinois 60439, USA*

<sup>c</sup>*Department of Physics and Astronomy, Northwestern University, Evanston, Illinois 60208, USA*

<sup>d</sup>*Theoretical Division, Los Alamos National Laboratory, Los Alamos, NM, 87545, USA*

---

## Abstract

Deep inelastic scattering on nuclei at the Electron-Ion Collider will open new opportunities to investigate the structure of matter. Heavy flavor-tagged jets are complementary probes of the partonic composition and transport coefficients of large nuclei, but introduce a new mass scale that modifies the structure of parton showers and must be carefully accounted for in perturbative calculations. In the framework of soft-collinear effective theory with Glauber gluon interactions, we present the first calculation of inclusive charm-jet and bottom-jet cross sections in electron-nucleus collisions at next-to-leading order and compare them to the reference electron-proton case. We also show predictions for the heavy flavor-tagged jet momentum sharing distributions to further clarify the correlated in-medium modification of jet substructure.

---

## 1. Introduction

In the past several years significant progress has been made toward defining the physics of the future Electron-Ion Collider (EIC) and establishing detector requirements that will enable the proposed measurements. The recently released Yellow Report [1] is an important first step in summarizing the current status of deep inelastic scattering (DIS) studies at the future facility, but is far from complete in terms of science reach. In the years that lead to EIC operation its physics program will continue to expand to reflect the pertinent new developments in theory and phenomenology. In this letter we report one such development - the first calculation of heavy flavor jet production and substructure in electron-nucleus (e+A) collisions.

Theoretical studies of charm-quark jets (c-jets) and bottom-quark jets (b-jets) in nucleus-nucleus (A+A) collisions [2–8] and related experimental measurements at the Large Hadron Collider [9–13] have become readily available. Heavy flavor-tagged jets will also soon be studied at the Relativistic Heavy Ion Collider (RHIC) [14] with the sPHENIX experiment. On one hand these results complement the physics of inclusive jets dominated by light partons in heavy ion collisions and provide alternative diagnostics of the transport properties of nuclear matter. On the other hand there are unique aspects of quantum chromodynamics (QCD) that can only be accessed with heavy flavor measurements. First and foremost is the effect of heavy quark mass on parton showers dubbed generically the “dead cone” effect [15]. It was found to play an important role in non-Abelian parton energy loss at small and moderate heavy quark energies [16–18] and in the full medium-induced splitting kernels [19–21] - the analogues of Altarelli-Parisi branching in nuclear matter. Second, in this kinematic regime, the heavy quark mass can produce quantitatively and even

---

*Email addresses:* haitao.li@sdu.edu.cn (Hai Tao Li), zelongliu@itp.unibe.ch (Ze Long Liu), ivitev@lanl.gov (Ivan Vitev)

qualitatively different modification of jet observables in reactions with nuclei in comparison to the massless case [3]. For an overview of heavy flavor physics, albeit with more emphasis on hadron production, see e.g. Refs. [22–24].

At the same time, theoretical studies of heavy flavor jets at the EIC have been extremely limited. In electron-proton (e+p) collisions c-jets produced in charge current reactions have been proposed [25] as a probe of the strangeness content of the proton at intermediate and large values of Bjorken- $x$ . The transverse spin asymmetry of back-to-back heavy flavor-tagged jet production has been shown to be sensitive to the gluon Sivers function [26]. Experimental feasibility studies for heavy flavor jet measurements at the EIC have also been performed [25, 27]. In electron-nucleus collisions this physics is not yet developed. Ref. [28] explored the possibility of using the total charm production cross section to constrain the gluon nuclear parton distribution function (nPDF). Semi-inclusive D-meson and B-meson production in DIS on nuclei can shed light on the physics of hadronization and differentiate between competing paradigms of hadron attenuation in cold nuclear matter [29, 30]. In this letter we take the studies of heavy flavor in cold nuclear matter to the next level and present predictions for c-jet and b-jet cross section and substructure modification in electron-nucleus collisions.

To address this problem we can take guidance from the recent calculation of light jet rates and the jet charge in DIS on nuclei [31]. Even in the absence of nuclear matter, the heavy quark mass  $m$  must be accounted for in perturbative calculations. It was introduced in Refs. [32, 33] in the framework of soft-collinear effective theory (SCET) [34–36] with focus on the  $m/p = \lambda \ll 1$  regime, yielding a new formulation with finite mass corrections SCET<sub>M</sub>. The role of the heavy quark mass in heavy flavor-tagged jet cross sections evaluated with the help of semi-inclusive jet functions (SiJFs) was also understood [4, 37]. In addition to the logarithms of the ratio of the hard scale  $\mu$  to the jet scale  $p_T R$  that should be resummed for small radii  $R$ , logarithms of the ratio of the jet scale to the heavy quark mass have also been accounted for. For reactions with nuclei, SCET<sub>M</sub> has been generalized to describe parton shower interactions in matter via the exchange of off-shell Glauber gluons [19]. This development, which resulted in the derivation of the in-medium splitting functions for heavy quarks, has been complemented by the re-analysis of parton branching using the formalism of lightcone wavefunctions [20], confirming earlier results and allowing to compute splittings in QCD media to any order in the opacity of matter. Last but not least, the contribution of medium-induced parton showers to the SiJFs for inclusive jets [38] and charm-quark jets / bottom-quark jets [4] has been derived, the latter being particularly relevant to this work. Here we show how this approach can be applied to deep inelastic scattering, and in particular to e+A reactions. We will complement the calculation of heavy flavor-tagged jet quenching in cold nuclear matter with the evaluation of the c-jet and b-jet soft-dropped momentum sharing distributions [39]. This observable is especially illuminating since its modification in QCD matter can be quite different at small and moderate transverse momenta relative to large ones, depending on the quark mass [3].

The rest of this letter is organized as follows: in Section 2 we present the theoretical formalism for calculating the b-jet and c-jet cross sections and the soft-dropped momentum sharing distributions in e+p and e+A reactions. Phenomenological results for DIS on a gold (Au) nucleus are shown in Section 3. We conclude in Section 4.

## 2. Theoretical Framework

### 2.1. Semi-inclusive jet cross sections at the EIC

The factorization formula for the cross section for semi-inclusive jet production in collinear leading-twist perturbative QCD can be written as [40]:

$$E_J \frac{d^3\sigma}{d^3P_J} = \frac{1}{S} \sum_{i,f} \int_0^1 \frac{dx}{x} \int_0^1 \frac{dz}{z^2} f^{i/N}(x, \mu) J_{J_Q/f}(z, p_T R, m, \mu) \left[ \hat{\sigma}_{i \rightarrow f} + f_{\text{ren}}^{\gamma/\ell} \left( \frac{-t}{s+u}, \mu \right) \hat{\sigma}^{\gamma i \rightarrow f} \right]. \quad (1)$$

Here  $f^{i/N}$  is the parton distribution function (PDF) of parton  $i$  in nucleon  $N$  and  $J_{J_Q/f}$  is the SiJF from parton  $f$  to jet  $J_Q$  containing heavy flavor.  $z$  and  $m$  denote the momentum fraction taken by the jet and the mass of the heavy flavor parton, respectively.  $p_T$  and  $R$  are the transverse momentum and radius of the semi-inclusive jet.  $\hat{\sigma}^{i \rightarrow f}$  denotes the cross section for lepton-parton scattering with initial-state parton  $i$  and final-state parton  $f$ . Lastly  $s, t, u$  are the partonic Mandelstam variables defined as  $s = (k + l)^2$ ,  $t = (k - p)^2$  and  $u = (l - p)^2$ , where  $l^\mu, k^\mu$  and  $p^\mu$  are the momenta of the incoming lepton, the incoming parton and the fragmenting parton, respectively. Because kinematic constraints on the scattered lepton are not employed in jet production at the EIC, events with forward lepton scattering can be selected. In this case, the hard process can be described by an incoming quasi-real photon scattering:  $\gamma q \rightarrow q(g)$ ,  $\gamma q \rightarrow g(q)$ ,  $\gamma g \rightarrow q(\bar{q})$ , which contributes to the cross section starting at order  $\alpha_{\text{EM}}^2 \alpha_s$ . Quasi-real photons originate from the incoming lepton and can be accurately described by the well known Weizsäcker-Williams (WW) distribution with a perturbative distribution function  $f_{\text{ren}}^{\gamma/\ell}(y, \mu)$  [41–44]. The analytical expressions for  $\hat{\sigma}^{i \rightarrow f}$ ,  $\hat{\sigma}^{\gamma i \rightarrow f}$  and  $f_{\text{ren}}^{\gamma/\ell}(y, \mu)$  up to  $\mathcal{O}(\alpha_{\text{EM}}^2 \alpha_s)$  can be found in [40]. We note that there is also a resolved photon contribution, related to the partonic content of the  $\gamma$  [45]. Formally, it starts at  $\mathcal{O}(\alpha_{\text{EM}}^2 \alpha_s^2)$  which is homogeneous with NNLO QCD corrections [46] and contributes at relatively small transverse momenta. Furthermore, the overall cross section normalization of high transverse momentum jets will cancel in the nuclear modification ratio that we study in Section 3. For these reasons, we did not consider the resolved photon component here and defer its investigation to future studies.

The NLO SiJFs for heavy flavor jets can be found in Ref. [37]. The evolution of heavy flavor SiJFs is briefly reviewed below. Since the heavy quark mass does not affect the ultraviolet (UV) behavior of diagrams, the evolution of heavy-flavor SiJFs obeys DGLAP-like equations similar to the ones for light-flavor SiJFs. The renormalization-group equation (RGE) is given by

$$\frac{d}{d \ln \mu^2} \begin{pmatrix} J_{J_Q/s}(x, \mu) \\ J_{J_Q/g}(x, \mu) \end{pmatrix} = \frac{\alpha_s}{2\pi} \int_x^1 \frac{dz}{z} \begin{pmatrix} P_{qq}(z) & 2P_{gq}(z) \\ P_{qg}(z) & P_{gg}(z) \end{pmatrix} \cdot \begin{pmatrix} J_{J_Q/s}(x/z, \mu) \\ J_{J_Q/g}(x/z, \mu) \end{pmatrix}, \quad (2)$$

where  $s = Q + \bar{Q}$ . Here,  $P_{ij}$  are usual Altarelli-Parisi splitting functions. To solve the above RGE, we work in Mellin moment space following the method outlined in [47]

$$J_{Q/g}(N) = \int_0^1 dz z^{N-1} J_{Q/g}(z). \quad (3)$$

The solution for the jet function in this space is given by

$$\begin{pmatrix} J_{J_Q/s}(N, \mu) \\ J_{J_Q/g}(N, \mu) \end{pmatrix} = \left[ e_+(N) \left( \frac{\alpha_s(\mu)}{\alpha_s(\mu_J)} \right)^{-r_-(N)} + e_-(N) \left( \frac{\alpha_s(\mu)}{\alpha_s(\mu_J)} \right)^{-r_+(N)} \right] \cdot \begin{pmatrix} J_{J_Q/s}(N, \mu_J) \\ J_{J_Q/g}(N, \mu_J) \end{pmatrix}, \quad (4)$$

where  $r_+(N)$  and  $r_-(N)$  are the larger and smaller eigenvalue of the leading-order singlet evolution matrix,

$$r_{\pm}(N) = \frac{1}{2\beta_0} \left[ P_{qq}(N) + P_{gg}(N) \pm \sqrt{(P_{qq}(N) - P_{gg}(N))^2 + 4P_{qg}(N)P_{gq}(N)} \right]. \quad (5)$$

The projector matrices  $e_{\pm}(N)$  in (4) are defined as

$$e_{\pm}(N) = \frac{1}{r_{\pm}(N) - r_{\mp}(N)} \begin{pmatrix} P_{qq}(N) - r_{\mp}(N) & 2N_f P_{gq}(N) \\ P_{qg}(N) & P_{gg}(N) - r_{\mp}(N) \end{pmatrix}. \quad (6)$$

Eventually, the evolved SiJFs in  $z$ -space can be obtained by performing an inverse Mellin transformation.

$$J_{J_Q/g}(z, \mu) = \frac{1}{2\pi i} \int_{C_N} dN z^{-N} J_{J_Q/g}(N, \mu), \quad (7)$$

where we chose the contour in the complex  $N$  plane to the right of all the poles of  $J_{J_Q/g}(N, \mu)$ . The NLO medium corrections to the  $Q \rightarrow J_Q$  and  $g \rightarrow J_Q$  SiJFs are similar to the case of heavy-ion collisions [4] and can be written as

$$\begin{aligned} J_{J_Q/Q}^{\text{med},(1)}(z, p_T R, m, \mu) &= \int_{z(1-z)p_T R}^{\mu} d^2 q_{\perp} f_{Q \rightarrow Q+g}^{\text{med}}(z, m, q_{\perp}) - \delta(1-z) \int_0^1 dx \int_{x(1-x)p_T R}^{\mu} d^2 q_{\perp} f_{Q \rightarrow Q+g}^{\text{med}}(x, m, q_{\perp}) \\ &= \left[ \int_{z(1-z)p_T R}^{\mu} d^2 q_{\perp} f_{Q \rightarrow Q+g}^{\text{med}}(z, m, q_{\perp}) \right]_+, \end{aligned} \quad (8)$$

and

$$J_{J_Q/g}^{\text{med},(1)}(z, p_T R, m, \mu) = \left[ \int_{z(1-z)p_T R}^{\mu} d^2 q_{\perp} f_{g \rightarrow Q+\bar{Q}}^{\text{med}}(z, m, q_{\perp}) \right]_+ + \int_{z(1-z)p_T R}^{\mu} d^2 q_{\perp} f_{g \rightarrow Q+\bar{Q}}^{\text{med}}(z, m, q_{\perp}), \quad (9)$$

respectively. Here  $f_{i \rightarrow j+k}^{\text{med}}$  is the medium induced splitting kernel. The scale  $\mu$  was introduced as a UV cut-off for the medium corrections [4, 38] which is set to be the jet transverse momentum in this work. In the presence of a QCD medium, it was demonstrated that the vacuum splitting must be replaced by the full splitting kernels for each possible branching channel

$$\frac{dN^{\text{full}}}{dz d^2 q_{\perp}} = \frac{dN^{\text{vac}}}{dz d^2 q_{\perp}} + f^{\text{med}}(z, m, q_{\perp}). \quad (10)$$

Hence, the full in-medium SiJFs are obtained as

$$J_{J_Q/i} = J_{J_Q/i}^{\text{vac}} + J_{J_Q/i}^{\text{med}}, \quad (11)$$

where the vacuum contributions are calculated at the LL accuracy, while only the fixed-order medium corrections are included consistently.

## 2.2. Soft-dropped jet momentum sharing distribution

Jet substructure is a promising to study the mass effects in parton shower evolution. In this work, we focus on the jet momentum sharing variable based on the “soft drop grooming” [48] in  $1 \rightarrow 2$  QCD splitting processes. It is defined as the distribution of

$$z_g = \frac{\min(p_{T1}, p_{T2})}{p_{T1} + p_{T2}}, \quad z_g > z_{\text{cut}}, \quad (12)$$

where  $p_{T1}$  and  $p_{T2}$  are the transverse momenta of the subjects in a reconstructed jet. For the heavy-flavor jet, we are interested in the kinematic region where the jet energy is much larger than the heavy quark mass,  $0 < m \ll p_T$ .

Consider an off-shell parton of momentum  $[p^+, p^-, \mathbf{0}_\perp]$ , with  $p^+$  the large lightcone component, that splits into two daughter partons  $[zp^+, q_\perp^2/zp^+, \mathbf{q}_\perp]$  and  $[(1-z)p^+, q_\perp^2/(1-z)p^+, -\mathbf{q}_\perp]$ . The massive splitting kernel  $Q \rightarrow Qg$ , for example, in the vacuum reads

$$\left(\frac{dN^{\text{vac}}}{dzd^2q_\perp}\right)_{Q \rightarrow Qg} = \frac{\alpha_s}{2\pi^2} \frac{C_F}{q_\perp^2 + z^2m^2} \left( \frac{1 + (1-z)^2}{z} - \frac{2z(1-z)m^2}{q_\perp^2 + z^2m^2} \right). \quad (13)$$

Here  $C_F$  is the quadratic Casimir invariant of the fundamental representation of SU(3). For  $q_\perp \gg m$  Eq. (13) reduces to the massless splitting functions, however when  $q_\perp \leq zm$  the heavy quark mass will significantly modify the momentum sharing observable - an effect that is amplified in nuclear matter [3]. If  $r_g$  is the angular separation between the subjets and  $p_T$  is the transverse momentum, then  $q_\perp = z(1-z)r_g p_T$  when  $r_g$  is not too large. The interesting regime discussed above can easily be reached with the moderate transverse momenta available at the EIC, especially for b-jets. Here, we start with the vacuum case to set up the stage for the jet splitting function calculation in heavy ion collisions. After soft-drop grooming in the parton branching  $i \rightarrow jk$ , the  $\theta_g$  and  $z_g$  distribution for parton  $i$  is

$$\left(\frac{dN^{\text{vac}}}{dz_g d\theta_g}\right)_i = \frac{\alpha_s}{\pi} \frac{1}{\theta_g} \sum_j P_{i \rightarrow jk}^{\text{vac}}(z_g), \quad (14)$$

with  $r_g = \theta_g R$ ,  $R$  being the jet radius. Resummation is necessary in the kinematic region with large splitting probability. It was performed to modified leading-logarithmic (MLL) accuracy in Ref. [48]. The resummed distribution for a  $i$ -type jet, initiated by a quark or a gluon, is

$$\frac{dN_i^{\text{vac,MLL}}}{dz_g d\theta_g} = \sum_j \left(\frac{dN^{\text{vac}}}{dz_g d\theta_g}\right)_{i \rightarrow jk} \exp \left[ - \int_{\theta_g}^1 d\theta \int_{z_{\text{cut}}}^{1/2} dz \sum_i \left(\frac{dN^{\text{vac}}}{dz d\theta}\right)_{i \rightarrow jk} \right]. \quad (15)$$

The normalized joint probability distribution then reads

$$p(\theta_g, z_g)|_i = \frac{dN_i^{\text{vac,MLL}}}{dz_g d\theta_g} \bigg/ \int_0^1 d\theta \int_{z_{\text{cut}}}^{1/2} dz \frac{dN_i^{\text{vac,MLL}}}{dz d\theta}, \quad (16)$$

and in for e+A collisions the corresponding medium contribution must be included according to Eq. (10).

### 3. Numerical results

#### 3.1. Semi-inclusive heavy flavor jet cross section modification in e+A relative to e+p at the EIC

In this section we present the main result of this work - heavy flavor jet cross section modification at the EIC. Here we consider two benchmark energy combinations for electron-proton collisions (for electron-nucleus collisions, the beam energy is per nucleon): 10 GeV (e)  $\times$  100 GeV (A) and 18 GeV (e)  $\times$  275 GeV (A).

In the following numerical calculations we use CT10nlo PDF sets [49] for the proton and the nCTEQ15 PDF sets [50] for the nucleus, and the associated strong coupling provided by LHAPDF6 [51]. The medium-induced splitting kernel up to first order of opacity [19, 21, 52] were used, consistent with earlier EIC studies [29, 31]. As a default choice, the nominal transport coefficient of cold nuclear matter for quarks is set to be  $\langle q_\perp^2 \rangle / \lambda_q = 0.05 \text{ GeV}^2/\text{fm}$  from the above references. The theoretical uncertainties in this section are evaluated by varying the transport parameter up and down by a factor of two, which represents the sensitivity of the observable to the transport coefficient.

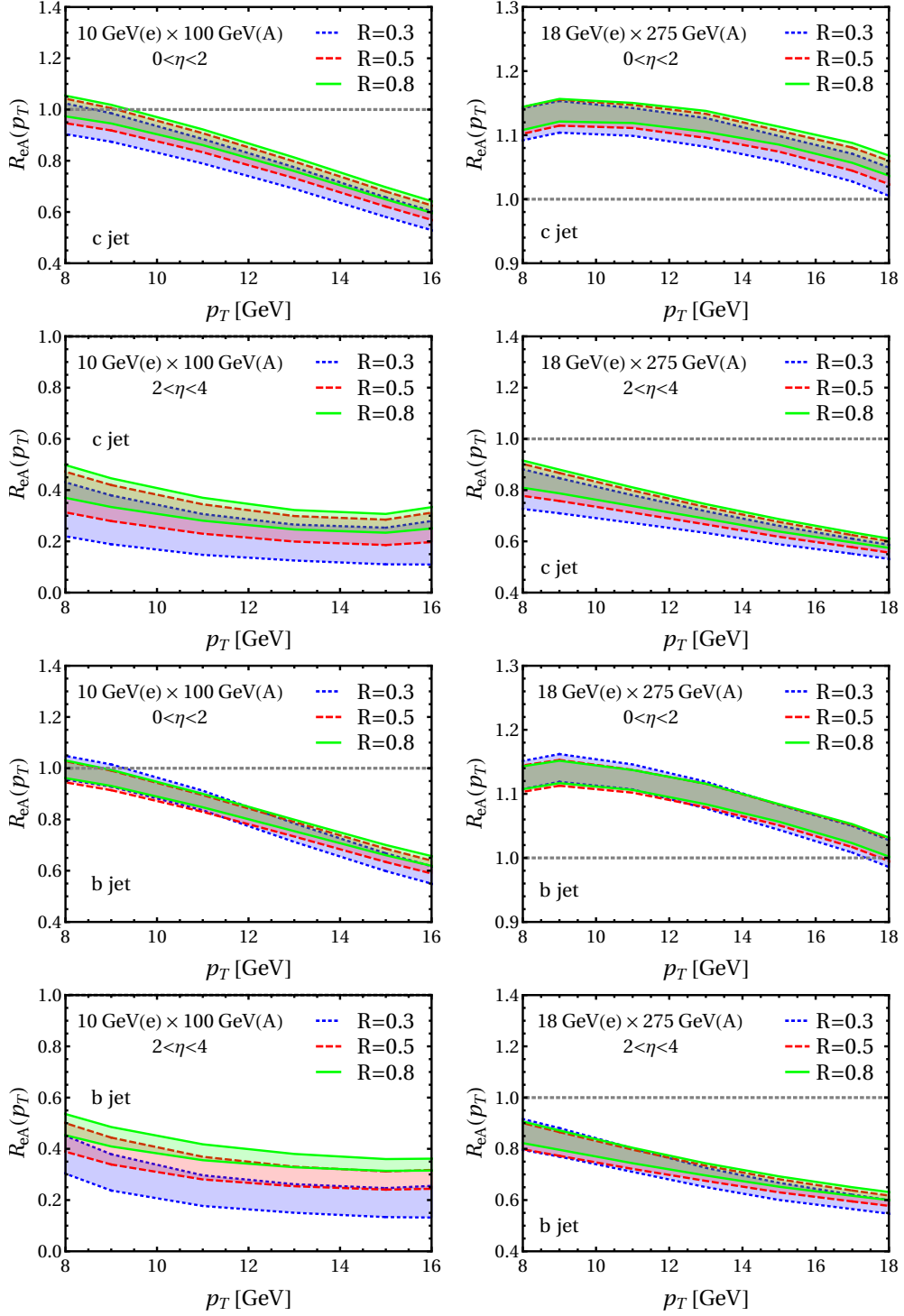


Figure 1: In-medium corrections for charm-quark jets and bottom-quark jets as a function of  $p_T$  at the EIC in two rapidity regions. Green bands (solid lines), red bands (dashed lines), and blue bands (dotted lines) correspond to  $R = 0.8$ ,  $R = 0.5$  and  $R = 0.3$ , respectively. Results for 10 GeV(e)  $\times$  100 GeV(A) collisions are shown on the left and results for 18 GeV(e)  $\times$  275 GeV(A) collisions are shown on the right.

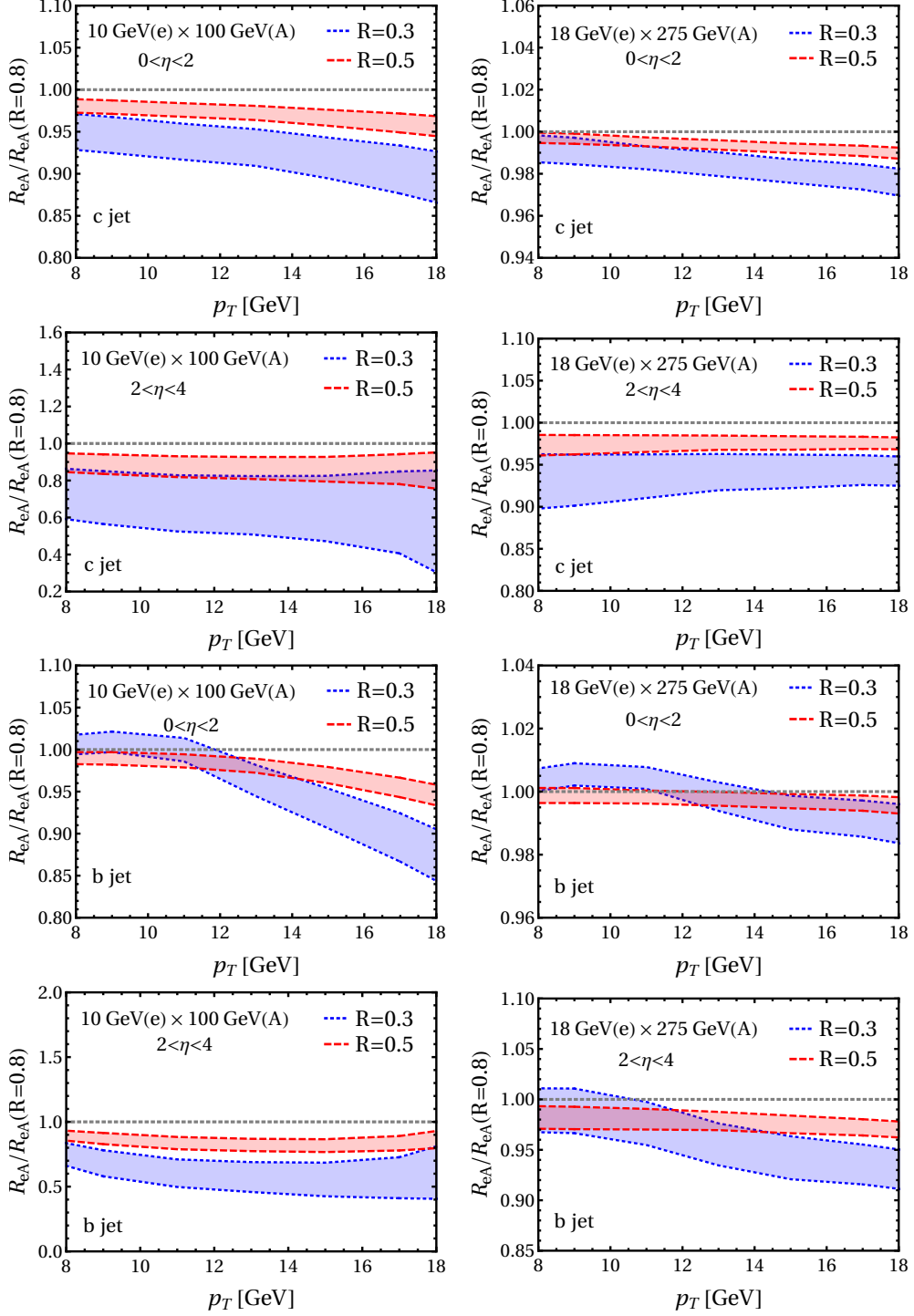


Figure 2: The ratio of  $R_{eA}$  normalized by  $R_{eA}(R=0.8)$  for c-jets and b-jets as a function of  $p_T$  at the EIC. Blue bands (dotted lines) and red bands (dashed lines) correspond to  $R=0.3$  and  $R=0.5$ , respectively. The kinematic regions and beam energy combinations are as in Fig. (1).

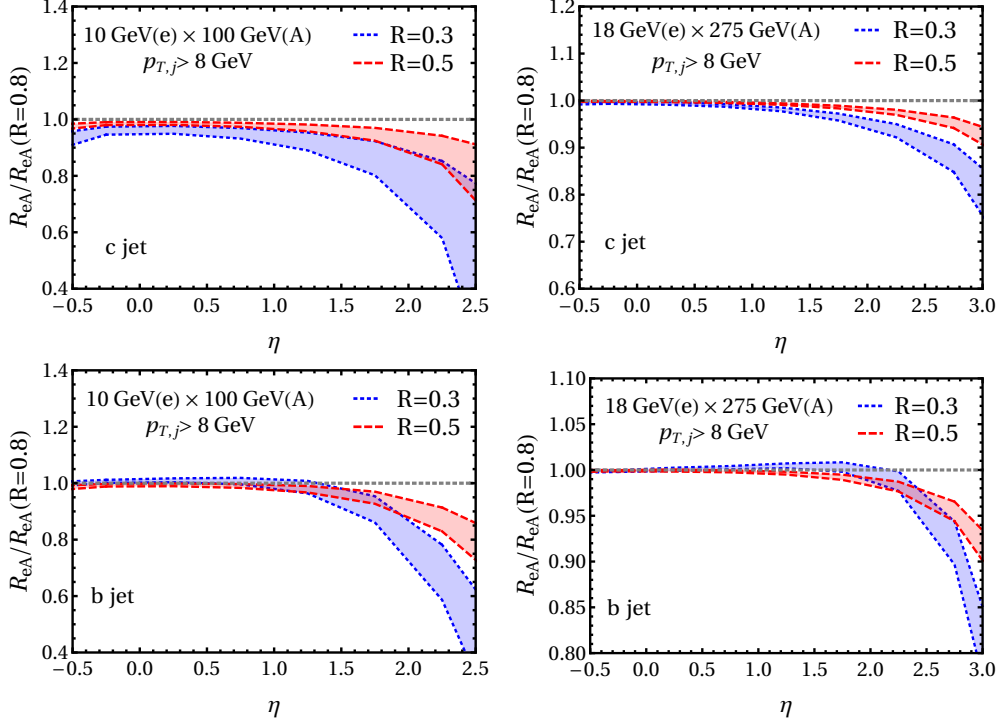


Figure 3: The ratio of  $R_{eA}$  normalized by  $R_{eA}(R=0.8)$  for heavy flavor jet production as a function of  $\eta$  at the EIC. Blue bands (solid lines) and red bands (dashed lines) correspond to  $R=0.3$  and  $R=0.5$ , respectively.

To investigate the nuclear medium effects, we study the ratio of the cross sections in electron-gold (e+Au) collisions normalized by the number of nucleons to the one in e+p collisions.

$$R_{eA}(R) = \frac{1}{A} \int \frac{d\sigma}{d\eta dp_T} \Big|_{e+Au} d\eta \Bigg/ \int \frac{d\sigma}{d\eta dp_T} \Big|_{e+p} d\eta. \quad (17)$$

In Figs. 1 we present  $R_{eA}$  for c-jets and b-jets as a function of the transverse momentum  $p_T$  in the laboratory frame in two rapidity bins  $0 < \eta < 2$  and  $2 < \eta < 4$ . The left column of panels is for 10 GeV  $\times$  100 GeV e+Au collision and the right column of panels is for 18 GeV  $\times$  275 GeV ones. The in-medium shower corrections induced by the interactions between the final-state partons and the nucleus vary with the parton energy in the nuclear rest frame, where the lower energy parton receives larger medium corrections. Therefore, in the forward (nucleus-going) rapidity region  $2 < \eta < 4$  we can see more significant jet quenching due to final-state interactions in the large nucleus. Furthermore, a clear separation of jet suppression is observed as a function of the radius  $R$ . Initial-state effects reflecting the difference between proton and nuclear PDFs also play an important role in  $R_{eA}$ . In the kinematic domains that we consider the smaller beam energies combination is primarily sensitive to the so called EMC region. At the higher beam energies combination we see a clear transition from the anti-shadowing region near midrapidity to the EMC at forward rapidity. Initial-state effects are large for c-jets and b-jets as their production channels are dominated by gluon and sea quarks.

To understand the structure and evolution of showers containing heavy quarks in cold nuclear matter and to use them as tomographic probes at the EIC, it is essential to reduce the effects of nPDFs and enhance the effects of final-state interactions. A successful strategy was developed on the example of inclusive light parton jets [29] and it involves measuring the ratio of the modifications with different jet radii, e.g.



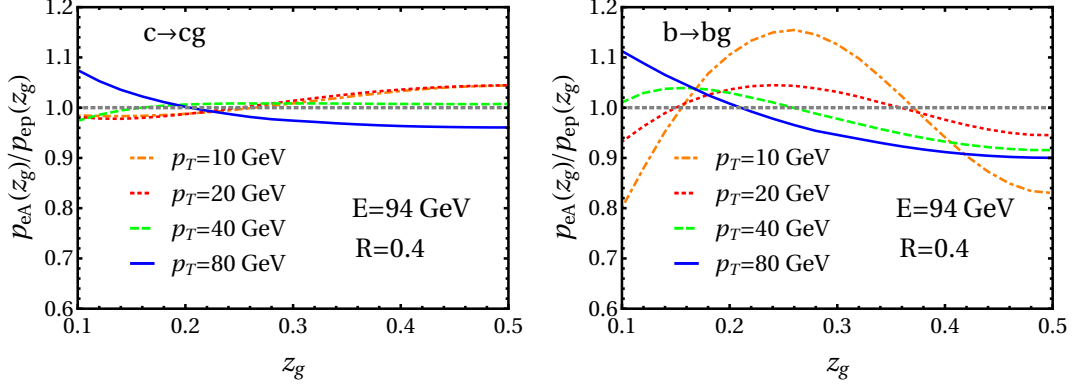


Figure 4: The modification of the jet splitting functions for  $c \rightarrow cg$  (left) and  $b \rightarrow bg$  (right). The energy of the jet is fixed at 94 GeV at the rest frame of the nucleus. The orange dot-dashed, red dotted, green dashed and blue solid lines denote the distribution with  $p_T = 10$  GeV, 20 GeV, 40 GeV and 80 GeV, respectively.

$R_{eA}(R)/R_{eA}(R = 0.8)$ . In such double ratio initial-state effects in e+A reactions will cancel for jets with a similar kinematics. This double ratio is also an observable sensitive to the angular distribution of in-medium branching processes [31, 53]. Furthermore, it provides an opportunity to explore smaller center-of-mass energies where the final-state effects are expected to be sizable even though the cross section is small. Such measurements will take advantage of the high-luminosity design of the future facility. Our predictions for the double ratio of jet cross section suppression in two rapidity bins at the EIC are presented in Fig. 2, where the left and right panels correspond to the results for 10 GeV (e)  $\times$  100 GeV (A) and 18 GeV (e)  $\times$  275 GeV (A) collisions. The blue and red bands correspond to jet radii  $R = 0.3$  and  $0.5$ , respectively, with the large normalization radius  $R = 0.8$  and with variation of the cold nuclear matter transport coefficient. Since medium-induced parton showers are broader than the ones in the vacuum, for smaller jet radii the suppression from final-state interactions is more significant. For both c-jets and b-jets, we can identify larger in-medium effects at 10 GeV  $\times$  100 GeV e+Au collision than at 18 GeV  $\times$  275 GeV collision with the same  $p_T$  range fixed. In fact, these are as large as the ones observed for light jets. Additionally, jet production in the forward rapidity region  $2 < \eta < 4$  receives the largest in-medium corrections.

We flesh out the rapidity dependence of  $R_{eA}$  in Fig. 3. Instead of rapidity, we have integrated the  $p_T$ -dependent cross sections above 8 GeV. Once again we show 10 GeV  $\times$  100 GeV (left) and 18 GeV  $\times$  275 GeV e+Au collisions (right). The upper and bottom two panels correspond to c-jets and b-jets, respectively. It is very clear that the medium-induced suppression is much enhanced in the forward rapidity region where the jet has smaller energy in the nuclear rest frame - a region that should be well-instrumented for these key measurements at the EIC.

### 3.2. Heavy flavor-tagged jet substructure

The jet splitting-function observable in e+A, i.e. the distribution of  $z_g$ , only depends on the final-state interactions between the jet and cold nuclear matter. At the EIC we probe a regime very different from heavy ion collisions. To illustrate this we study the  $p_T$  dependence of  $p_{eA}(z_g)/p_{ep}(z_g)$  and fix the jet energy in the rest frame of the nucleus to be 94 GeV for a jet radius  $R = 0.4$ . With the design energies, the transverse momentum of jets at EIC for practical purposes will be limited to about 30 GeV. However, a much larger range of jet transverse momentum  $10 < p_T < 80$  GeV is used here to demonstrate the  $p_T$

dependence and compare the large  $p_T$  region with the previous analyses in Ref. [3].<sup>1</sup> The results for charm-quark jets (left) and bottom-quark jets (right) are presented in Fig. 4 for the nominal value of the medium's transport parameter. Even though at large jet  $p_T$  the modifications of c-jet and b-jet substructure are similar because  $m \ll p_T$ , we are beginning to see hints of the quark mass effect. When  $p_T \sim E$ , the results have a qualitatively similar behavior with the  $z_g$  modifications in heavy-ion collisions [3]. For the small jet  $p_T$  a much larger mass effect is observed by comparing the c-jet and b-jet modifications. Not only is the magnitude larger for the bottom quark-initiated ones, but the shape of the modification differs consistent with the fact that the scale  $z_g m$  plays an important role in the branching Eq. (13).

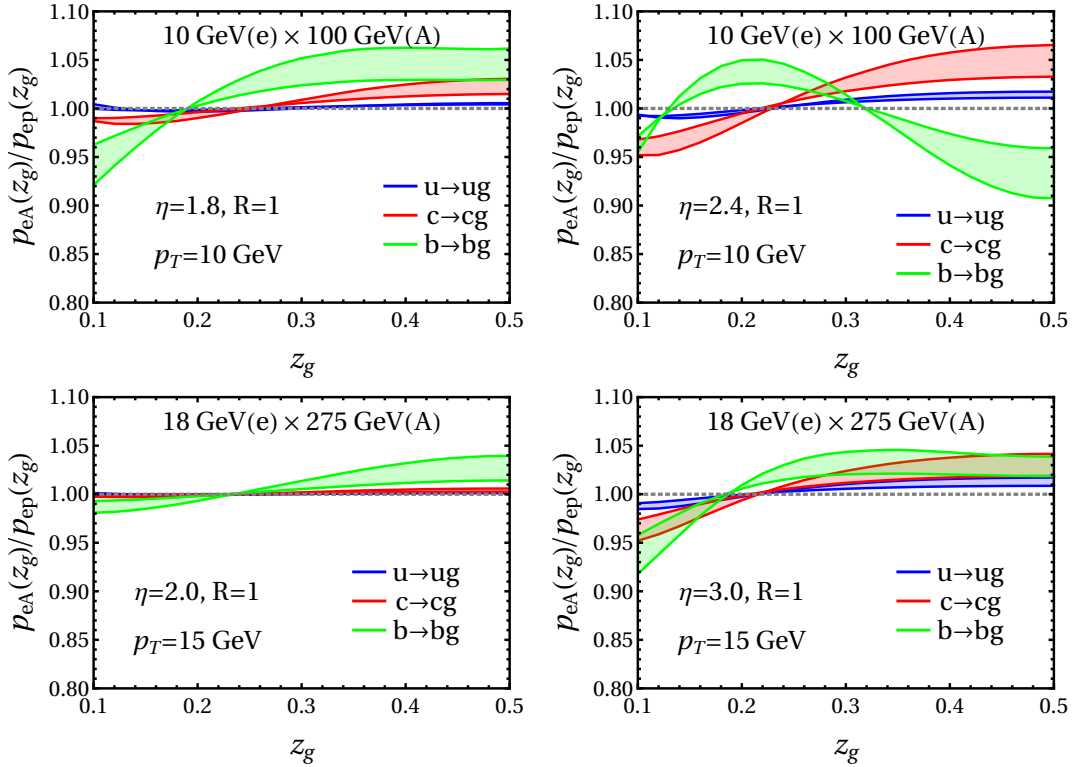


Figure 5: The modification of the jet splitting functions for c-jets and b-jets vs  $z_g$  at the EIC. The upper and bottom two panels correspond to the result for 10 GeV  $\times$  100 GeV and 18 GeV  $\times$  275 GeV e+Au to e+p collisions, respectively. The jet radius  $R = 1$  and two different rapidities are presented for each energy combination.

In Fig. 5, we present the modification of the jet splitting functions for charm jets and bottom jets with fixed jet rapidity at the EIC. Upper panels correspond to the results for 10 GeV  $\times$  100 GeV collisions and bottom panels correspond to the results 18 GeV  $\times$  275 GeV collisions, respectively. The jet radius is chosen to be  $R = 1$ , thus there is still available, albeit limited, phase space to ensure  $m \ll p_T R$ . The blue, red and green bands correspond to our calculations for light, c-quark and b-quark jets, respectively, and the bands reflect the uncertainties to the variation of the transport parameter by a factor of two. It is clear that, just as in the case of the cross sections, the in-medium corrections are larger in the forward rapidity region of the jet, because the corresponding jet energy in the rest frame of the nucleus is smaller. At the transverse

<sup>1</sup>It is completely clear that the higher transverse momenta shown cannot be reached at EIC kinematics. That would be possible in heavy ion collisions. We ignore kinematic constraints to make a physics point.

momenta accessible at the EIC the modification is quite different when compared to heavy ion collisions. By changing rapidity we can also see a difference in the modification pattern of bottom-quark jets which we attribute to the interplay between mass and parton energy in the non-Abelian Landau-Pomeranchuk-Migdal (LPM) effect for heavy quarks. These findings are intriguing and, clearly, more detailed future studies of heavy flavor-tagged jet substructure at the EIC will be quite important.

#### 4. Conclusions

In summary, we presented the first calculation of semi-inclusive charm-quark jet and bottom-quark jet production and substructure in e+A relative to e+p collisions at the EIC. Our formalism allowed to obtain NLO results by consistently combining the parton level cross sections and semi-inclusive jet functions up to NLO, and included resummation for small jet radii in electron-hadron reactions. We found that heavy flavor-tagged jet production is more sensitive to the gluon and sea quark distributions in nucleons and nuclei in comparison to light jets. Thus, in kinematic regions where  $R_{eA}$  is dominated by initial-state nPDF effects the modification was even stronger when compared to inclusive jets. Similar to the case of light jets, by applying the strategy of studying ratios of the nuclear modification with two different jet radii we were successful in eliminating nPDF effects, primarily the anti-shadowing and the EMC effect in the regions of interest. The remaining quenching of the jet spectra can be as large as a factor of two for small jet radii, for example  $R = 0.3$ , and can clearly be attributed to final-state interactions and in-medium modification of parton showers containing heavy quarks. This suppression is comparable to the one predicted for light jets and expected to be observed in the proton/nucleus going direction. In contrast, near mid rapidity and at backward rapidity the deviation of  $R_{eA}(R)/R_{eA}(R = 0.8)$  from unity is small since the energy of the parton/jet in the rest frame of the nucleus is very large. This, in turn, strongly reduces the contribution of in-medium parton shower due to the non-Abelian LPM effect. In fact, even at forward rapidity and smaller center-of-mass energies the parton energies in nuclear rest frame are quite sizeable and, therefore, there isn't much difference in the suppression of c-jets and b-jets.

We complemented the calculation of semi-inclusive jet cross sections with a calculation of the groomed, soft-dropped momentum sharing distribution. Our results show that the substructure modification in e+A relative to e+p reactions is relatively small – on the order of 10% or smaller. Still, just like in the case of heavy ion collisions at relatively small transverse momenta the differences in the subjet distribution are most pronounced for b-jets, followed by c-jets. In the kinematic regime accessible at the EIC the modification of light jets was found to be the smallest. In contrast to the heavy ion case, however, there is significant difference between the energy of the parton in the rest frame of the nucleus and the jet scale which determines the available phase space for substructure even for large radii  $R \sim 1$ . Thus, the jet momentum sharing distribution at the EIC probes a different interplay between the heavy quark mass and suppression of small-angle medium-induced radiation – a regime that can only be accessed at the EIC and merits further investigation in the future. We conclude by pointing out that with the theoretical tools that are becoming available one can also look at how subeikonal corrections to in-medium branching, such as the effects of varying matter density [54], propagate into the observables that we predicted in this work.

#### Acknowledgments

This work was supported by the U.S. Department of Energy under Contract No. 89233218CNA000001, the Los Alamos National Laboratory LDRD program, and the TMD topical collaboration for nuclear theory. H.T. Li is supported by the U.S. Department of Energy under Contract No. DE-AC02-06CH11357 and the National Science Foundation under Grant No. NSF-1740142.

## References

- [1] R. Abdul Khalek et al., *Science Requirements and Detector Concepts for the Electron-Ion Collider: EIC Yellow Report*, 2103.05419.
- [2] J. Huang, Z.-B. Kang and I. Vitev, *Inclusive b-jet production in heavy ion collisions at the LHC*, *Phys. Lett. B* **726** (2013) 251–256, [1306.0909].
- [3] H. T. Li and I. Vitev, *Inverting the mass hierarchy of jet quenching effects with prompt b-jet substructure*, *Phys. Lett. B* **793** (2019) 259–264, [1801.00008].
- [4] H. T. Li and I. Vitev, *Inclusive heavy flavor jet production with semi-inclusive jet functions: from proton to heavy-ion collisions*, *JHEP* **07** (2019) 148, [1811.07905].
- [5] Z.-B. Kang, J. Reiten, I. Vitev and B. Yoon, *Light and heavy flavor dijet production and dijet mass modification in heavy ion collisions*, *Phys. Rev. D* **99** (2019) 034006, [1810.10007].
- [6] S. Wang, W. Dai, B.-W. Zhang and E. Wang, *Diffusion of charm quarks in jets in high-energy heavy-ion collisions*, *Eur. Phys. J. C* **79** (2019) 789, [1906.01499].
- [7] W. Fan, W. Ke and S. A. Bass, *Heavy jet analysis within the JETSCAPE framework*, *PoS High-pT2019* (2020) 033.
- [8] L. Dai, C. Kim and A. K. Leibovich, *Heavy quark jet production near threshold*, *JHEP* **09** (2021) 148, [2104.14707].
- [9] CMS collaboration, S. Chatrchyan et al., *Evidence of b-Jet Quenching in PbPb Collisions at  $\sqrt{s_{NN}} = 2.76$  TeV*, *Phys. Rev. Lett.* **113** (2014) 132301, [1312.4198].
- [10] CMS collaboration, V. Khachatryan et al., *Transverse momentum spectra of inclusive b jets in pPb collisions at  $\sqrt{s_{NN}} = 5.02$  TeV*, *Phys. Lett. B* **754** (2016) 59, [1510.03373].
- [11] CMS collaboration, A. M. Sirunyan et al., *Measurements of the charm jet cross section and nuclear modification factor in pPb collisions at  $\sqrt{s_{NN}} = 5.02$  TeV*, *Phys. Lett. B* **772** (2017) 306–329, [1612.08972].
- [12] CMS collaboration, A. M. Sirunyan et al., *Studies of charm quark diffusion inside jets using PbPb and pp collisions at  $\sqrt{s_{NN}} = 5.02$  TeV*, *Phys. Rev. Lett.* **125** (2020) 102001, [1911.01461].
- [13] ALICE collaboration, A. I. Sheikh, *Measurements of heavy-flavor jets with ALICE at the LHC*, *Nucl. Part. Phys. Proc.* **309-311** (2020) 174–180, [2009.02751].
- [14] PHENIX collaboration, A. Adare et al., *An Upgrade Proposal from the PHENIX Collaboration*, 1501.06197.
- [15] Y. L. Dokshitzer and D. E. Kharzeev, *Heavy quark colorimetry of QCD matter*, *Phys. Lett. B* **519** (2001) 199–206, [hep-ph/0106202].
- [16] M. Djordjevic and M. Gyulassy, *Heavy quark radiative energy loss in QCD matter*, *Nucl. Phys. A* **733** (2004) 265–298, [nucl-th/0310076].
- [17] B.-W. Zhang, E. Wang and X.-N. Wang, *Heavy quark energy loss in nuclear medium*, *Phys. Rev. Lett.* **93** (2004) 072301, [nucl-th/0309040].
- [18] N. Armesto, C. A. Salgado and U. A. Wiedemann, *Medium induced gluon radiation off massive quarks fills the dead cone*, *Phys. Rev. D* **69** (2004) 114003, [hep-ph/0312106].
- [19] Z.-B. Kang, F. Ringer and I. Vitev, *Effective field theory approach to open heavy flavor production in heavy-ion collisions*, *JHEP* **03** (2017) 146, [1610.02043].
- [20] M. D. Sievert and I. Vitev, *Quark branching in QCD matter to any order in opacity beyond the soft gluon emission limit*, *Phys. Rev. D* **98** (2018) 094010, [1807.03799].
- [21] M. D. Sievert, I. Vitev and B. Yoon, *A complete set of in-medium splitting functions to any order in opacity*, *Phys. Lett. B* **795** (2019) 502–510, [1903.06170].
- [22] A. D. Frawley, T. Ullrich and R. Vogt, *Heavy flavor in heavy-ion collisions at RHIC and RHIC II*, *Phys. Rept.* **462** (2008) 125–175, [0806.1013].
- [23] A. Andronic et al., *Heavy-flavour and quarkonium production in the LHC era: from proton–proton to heavy-ion collisions*, *Eur. Phys. J. C* **76** (2016) 107, [1506.03981].
- [24] X. Dong, Y.-J. Lee and R. Rapp, *Open Heavy-Flavor Production in Heavy-Ion Collisions*, *Ann. Rev. Nucl. Part. Sci.* **69** (2019) 417–445, [1903.07709].
- [25] M. Arratia, Y. Furletova, T. J. Hobbs, F. Olness and S. J. Sekula, *Charm jets as a probe for strangeness at the future Electron-Ion Collider*, *Phys. Rev. D* **103** (2021) 074023, [2006.12520].
- [26] Z.-B. Kang, J. Reiten, D. Y. Shao and J. Terry, *QCD evolution of the gluon Sivers function in heavy flavor dijet production at the Electron-Ion Collider*, *JHEP* **05** (2021) 286, [2012.01756].
- [27] X. Li, *Heavy Flavor and Jet Studies for the Future Electron-Ion Collider to Explore the Hadronization Process*, in *28th International Workshop on Deep Inelastic Scattering and Related Subjects*, 7, 2021. 2107.09035.
- [28] E. Chudakov, D. Higinbotham, C. Hyde, S. Furletov, Y. Furletova, D. Nguyen et al., *Probing nuclear gluons with heavy quarks at EIC*, *PoS DIS2016* (2016) 143, [1608.08686].
- [29] H. T. Li, Z. L. Liu and I. Vitev, *Heavy meson tomography of cold nuclear matter at the electron-ion collider*, *Phys. Lett. B* **816** (2021) 136261, [2007.10994].

- [30] X. Li et al., *A New Heavy Flavor Program for the Future Electron-Ion Collider*, *EPJ Web Conf.* **235** (2020) 04002, [2002.05880].
- [31] H. T. Li and I. Vitev, *Nuclear Matter Effects on Jet Production at Electron-Ion Colliders*, *Phys. Rev. Lett.* **126** (2021) 252001, [2010.05912].
- [32] I. Z. Rothstein, *Factorization, power corrections, and the pion form-factor*, *Phys. Rev. D* **70** (2004) 054024, [hep-ph/0301240].
- [33] A. K. Leibovich, Z. Ligeti and M. B. Wise, *Comment on quark masses in SCET*, *Phys. Lett. B* **564** (2003) 231–234, [hep-ph/0303099].
- [34] C. W. Bauer, D. Pirjol and I. W. Stewart, *Soft collinear factorization in effective field theory*, *Phys. Rev.* **D65** (2002) 054022, [hep-ph/0109045].
- [35] C. W. Bauer, S. Fleming, D. Pirjol, I. Z. Rothstein and I. W. Stewart, *Hard scattering factorization from effective field theory*, *Phys. Rev. D* **66** (2002) 014017, [hep-ph/0202088].
- [36] M. Beneke, A. P. Chapovsky, M. Diehl and T. Feldmann, *Soft collinear effective theory and heavy to light currents beyond leading power*, *Nucl. Phys.* **B643** (2002) 431–476, [hep-ph/0206152].
- [37] L. Dai, C. Kim and A. K. Leibovich, *Heavy Quark Jet Fragmentation*, *JHEP* **09** (2018) 109, [1805.06014].
- [38] Z.-B. Kang, F. Ringer and I. Vitev, *Inclusive production of small radius jets in heavy-ion collisions*, *Phys. Lett.* **B769** (2017) 242–248, [1701.05839].
- [39] P. Ilten, N. L. Rodd, J. Thaler and M. Williams, *Disentangling Heavy Flavor at Colliders*, *Phys. Rev. D* **96** (2017) 054019, [1702.02947].
- [40] P. Hinderer, M. Schlegel and W. Vogelsang, *Single-Inclusive Production of Hadrons and Jets in Lepton-Nucleon Scattering at NLO*, *Phys. Rev. D* **92** (2015) 014001, [1505.06415].
- [41] C. von Weizsacker, *Radiation emitted in collisions of very fast electrons*, *Z. Phys.* **88** (1934) 612–625.
- [42] E. Williams, *Nature of the high-energy particles of penetrating radiation and status of ionization and radiation formulae*, *Phys. Rev.* **45** (1934) 729–730.
- [43] A. Bawa and W. Stirling, *Validity of the Equivalent Photon Approximation in High-energy Electron Proton Collisions*, *J. Phys. G* **15** (1989) 1339.
- [44] S. Frixione, M. L. Mangano, P. Nason and G. Ridolfi, *Improving the Weizsacker-Williams approximation in electron - proton collisions*, *Phys. Lett. B* **319** (1993) 339–345, [hep-ph/9310350].
- [45] C. Uebler, A. Schäfer and W. Vogelsang, *Direct- and Resolved-Photon Threshold Resummation for Polarized High- $p_T$  Hadron Production at COMPASS*, *Phys. Rev. D* **96** (2017) 074026, [1708.08284].
- [46] R. Boughezal, F. Petriello and H. Xing, *Inclusive jet production as a probe of polarized parton distribution functions at a future EIC*, *Phys. Rev. D* **98** (2018) 054031, [1806.07311].
- [47] A. Vogt, *Efficient evolution of unpolarized and polarized parton distributions with QCD-PEGASUS*, *Comput. Phys. Commun.* **170** (2005) 65–92, [hep-ph/0408244].
- [48] A. J. Larkoski, S. Marzani, G. Soyez and J. Thaler, *Soft Drop*, *JHEP* **05** (2014) 146, [1402.2657].
- [49] H.-L. Lai, M. Guzzi, J. Huston, Z. Li, P. M. Nadolsky, J. Pumplin et al., *New parton distributions for collider physics*, *Phys. Rev. D* **82** (2010) 074024, [1007.2241].
- [50] K. Kovarik et al., *nCTEQ15 - Global analysis of nuclear parton distributions with uncertainties in the CTEQ framework*, *Phys. Rev.* **D93** (2016) 085037, [1509.00792].
- [51] A. Buckley, J. Ferrando, S. Lloyd, K. Nordstrom, B. Page, M. Ruefenacht et al., *LHAPDF6: parton density access in the LHC precision era*, *Eur. Phys. J.* **C75** (2015) 132, [1412.7420].
- [52] G. Ovanessian and I. Vitev, *Medium-induced parton splitting kernels from Soft Collinear Effective Theory with Glauber gluons*, *Phys. Lett.* **B706** (2012) 371–378, [1109.5619].
- [53] I. Vitev, S. Wicks and B.-W. Zhang, *A Theory of jet shapes and cross sections: From hadrons to nuclei*, *JHEP* **11** (2008) 093, [0810.2807].
- [54] A. V. Sadofyev, M. D. Sievert and I. Vitev, *Ab initio coupling of jets to collective flow in the opacity expansion approach*, *Phys. Rev. D* **104** (2021) 094044, [2104.09513].